

# Effects of Replacement of Prolines with Alanines on the Catalytic Activity and Thermostability of Inorganic Pyrophosphatase from Thermophilic Bacterium PS-3<sup>1</sup>

Hideki Masuda,\* Toshio Uchiumi,\* Michiko Wada,\* Tetsuroh Ichiba,† and Akira Hachimori\*<sup>2</sup>

\*Institute of High Polymer Research, Faculty of Textile Science and Technology, Shinshu University, 3-15-1 Tokida, Ueda, Nagano 386-8567; and †Ohtsuka Pharmaceutical Co., Ltd., Analytical Development, Formulation Research Institute, Tokushima, Tokushima 771-1820

Received August 6, 2001; accepted October 23, 2001

Each of the 10 proline residues of the inorganic pyrophosphatase (PPase) subunit of thermophilic bacterium PS-3 (PS-3) was replaced with alanine by the PCR-mutagenesis method. The variants were classified into three groups according to the effects of the replacements on their catalytic activities in 20 mM Tris-HCl, pH 7.8, containing 5 mM MgCl<sub>2</sub>: the catalytic activity was (i) slightly affected (P39A and P69A), (ii) considerably reduced (P14A, P43A, P59A, and P116A), and (iii) completely or almost completely abolished (P72A, P100A, P104A, and P146A). HPLC-gel chromatography in the presence of 5 mM MgCl<sub>2</sub> revealed the following subunit assembly of the variants: group (i), a hexamer; group (ii), a hexamer or a mixture of a hexamer and a trimer, although the hexamer was predominant; and group (iii), a trimer or a monomer. The thermostability of the variant PPases depended upon the amount of hexamer remaining in the presence of Mg<sup>2+</sup> at high temperature. The results indicated that the hexamer state formed through protomer-protomer and trimer-trimer interactions is necessary for the PS-3 PPase to retain the correct structure for full catalytic activity and thermostability.

**Key words:** inorganic pyrophosphatase, mutagenesis, polymerase chain reaction, proline, thermophilic bacterium PS-3.

Inorganic pyrophosphatase [EC 3.6.1.1] specifically catalyzes the hydrolysis of pyrophosphate to orthophosphate. This reaction provides a thermodynamic pull for many biosynthetic reactions (1–3) and is essential for life (4–6). PPases require bivalent metal ions for catalysis, Mg<sup>2+</sup> conferring the highest activity. Based on their primary structures, soluble PPases can be divided into two families that exhibit no sequence similarity to each other.

Family I includes most of the currently known PPases (7). Family II, to which *Bacillus subtilis* PPase belongs, was discovered only recently (8–10), and all 19 of its proved or putative members are from bacteria (11). Family I can be further divided into prokaryotic, plant and animal/fungal PPases. The best-studied PPases are those from *Escherichia coli* and *Saccharomyces cerevisiae* in Family I, which have been extensively characterized by X-ray crystallography (12–16), and site-directed mutagenesis in combination with kinetic and thermodynamic measurements (17–23).

We previously determined, through studies involving Edman degradation (24) and cloning and expression of the gene (25), the primary structure of the PPase from thermophilic bacterium PS-3, which exhibits high sequence identity, including the evolutionarily well-conserved active-site residues, with the family I PPases (7). PS-3 PPase forms a hexamer derived from trimers in the presence of Mg<sup>2+</sup> to become enzymatically active and thermostable (26). Previously we reported that the newly formed interchain hydrogen bonds arising through the trimer-trimer interaction in the presence of Mg<sup>2+</sup> (>1 mM) partially contribute to the thermostability of PS-3 PPase (27), along with unknown mechanism(s) operating within the protein structure itself.

Proline residues restrict backbone bond rotation because of their pyrrolidine rings. Therefore, prolines are believed to decrease the entropy during protein unfolding by reducing the number of unfolded conformations that can be sampled by the protein (28). PS-3 PPase contains 10 proline residues per subunit. Based on the alignment of the primary structures of the 37 PPases of Family I (7), these proline residues in PS-3 PPase are classified into five groups: proline residues found in (i) all prokaryote, plant, and animal/fungal PPases [Pro-59 (34) and Pro-104 (26)], (ii) prokaryote and animal/fungal PPases [Pro-14 (30)], (iii) prokaryote and plant PPases [Pro-43 (28), Pro-69 (21), Pro-72 (23), and Pro-116 (20)], (iv) prokaryote PPases [Pro-39 (7) and Pro-100 (17)], and (v) only the PS-3, *Bacillus stearothermophilus* and *Solanum tuberosum* PPases [Pro-146] (the number in brackets after each proline residue indicates the number of

<sup>1</sup>This work was partially supported by Grants-in-Aid 10650782 and 13836004 for Scientific Research from the Ministry of Education, Science, Sports and Culture of Japan.

<sup>2</sup>To whom correspondence should be addressed. Tel: +81-268-21-5574, Fax: +81-268-21-5571, E-mail: AH43725@giptc.shinshu-u.ac.jp

Abbreviations: PPase, inorganic pyrophosphatase; PS-3, thermophilic bacterium PS-3; *Eco*, *Escherichia coli*; *Tth*, *Thermus thermophilus*; *Sac*, *Sulfolobus acidocaldarius*; *Tac*, *Thermoplasma acidophilum*; *Bst*, *Bacillus stearothermophilus*; CD, circular dichroism.

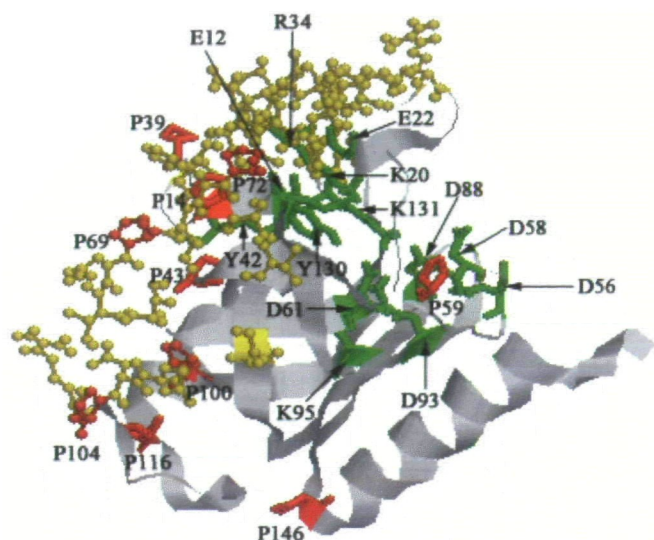


Fig. 1. **Structural model of the PPase from PS-3.** The model was constructed by homology modeling with the program package QUANTA/CHARMM. The X-ray structure of the *Tth* PPase served as a scaffold (26). Proline residues and active-site residues are shown in red and green, respectively. The protomer-protomer interface region (35) is shown in yellow.

PPases having that proline residue at the corresponding position among the 37 soluble PPase of Family I). Thus, these proline residues located at the corresponding positions are considered to be conserved evolutionarily, and they might play important roles in the integrity of the respective PPase structures, since the three-dimensional structures of the *E. coli* (*Eco*), *Thermus thermophilus* (*Tth*), and *Sulfolobus acidocaldarius* (*Sac*) PPases were reported to be quite similar to each other (29). The three-dimensional structure of the *Saccharomyces cerevisiae* PPase was also found to be similar to those of prokaryotic enzymes in spite of the little sequence similarity beyond the evolutionarily conserved residues of the active site and the different oligomeric organization (12). The three-dimensional structure of PS-3 PPase, predicted by computer analysis on homology modeling with the QUANTA/CHARMM program (Molecular Simulation) using the crystallographic data for the *Tth* PPase as a scaffold (30), is also very similar to those of both the *Eco* and *Tth* PPases (Fig. 1).

In the present study, site-directed mutagenesis of PS-3 PPase was conducted to replace each of the 10 proline residues with an alanine residue in order to determine its contribution to the structural integrity and thermostability of the enzyme.

#### MATERIALS AND METHODS

**Materials**—Restriction endonucleases, T4 DNA polymerase, Taq polymerase, a DNA ligation kit and Easytrap (gene clean kit) were purchased from Takara Shuzo. Antibiotics, egg-white lysozyme, ribonuclease A and low-gelling-temperature agarose (type S) were obtained from Nippon Gene. Phenyl-Sepharose CL4B, and TSK-gel Phenyl-5PW and TSK-gel G3000 SW were purchased from Pharmacia and Tosoh, respectively. All other chemicals were of analytical grade.

**Mutagenesis**—Oligonucleotide-directed mutagenesis was performed by the PCR-mutagenesis method with MUT 1 (Takara Shuzo) as the mutagenesis primer *in vitro*. The oligonucleotides used as primers were as follows: 5'-CT TCC GGT CGC AAT TTC G-3' (P14A), 5'-A AAA CAT CGC TGA ATA TAA GAC-3' (P39A), 5'-GTA TTC AGC CGC ATA AAA C-3' (P43A), 5'-T GTC GAG CGC GTC ACC A-3' (P59A), 5'-G GAA CGT CGC ATT TGT CG-3' (P69A), 5'-C GCA GCC CGC GAA CGT-3' (P72A), 5'-C TTC GAC CGC AAC GCC-3' (P100A), 5'-C AAA ACG CGC ATC TTC GAC-3' (P104A), 5'-T GTG CTG CGC GAG GTC-3' (P116A), and 5'-C TGC TTC CGC CCC CTC C-3' (P146A), the underlined nucleotides being the mutated Ala codons. A plasmid, pTTP3, containing the intact PS-3 *ppa* gene (25) was used as the template of the *ppa* gene manipulated in this work. pUC 118 was used as a vector for mutagenesis. JM109 was used as a host for the mutagenesis. Sequencing by the dideoxy chain-termination method (31) was performed to check the mutations.

**Purification of PPase**—*E. coli* JM109 cells expressing the wild-type and variant PS-3 PPases were produced by inoculating 1 liter of LB medium containing 80  $\mu$ M isopropyl  $\beta$ -D-thiogalactoside and 50  $\mu$ g/ml ampicillin with 2 ml of an overnight culture of the respective cells. Crude extracts of cells were obtained by grinding with  $Al_2O_3$  and extraction with 20 mM Tris-HCl buffer, pH 7.8, containing 5 mM  $MgCl_2$ . All PPases were purified to an electrophoretically homogeneous state according to the procedure reported previously (27). Samples were concentrated to approx. 10 mg/ml and then stored at  $-80^\circ C$ .

**Enzyme Assay**—PPase activity was determined by the procedure described previously (32). The assay medium contained 2 mM  $PP_i$ , 5 mM  $MgCl_2$ , 0.1 mM EDTA, and 50 mM Tris-HCl (pH 8.0) in a total volume of 0.5 ml. The reaction was initiated by adding 0.02 ml of enzyme solution, run for 10 min at  $37^\circ C$ , and arrested with 0.5 ml of 3% perchloric acid. The liberated phosphate was assayed by the method of Peel and Loghman (33). The protein concentration in a solution was determined with a Pierce bicinchromic acid protein assay kit, with BSA as the standard.

**Molecular Weight Estimation**—The molecular mass of PPase was determined by gel filtration. The protein solution (0.1 mg of protein in 100  $\mu$ l) was applied to an HPLC column of TSK-gel G3000SW (0.75 cm  $\times$  30 cm), then eluted with a buffer comprising 20 mM Tris-HCl, pH 7.8, in the presence of 5 mM  $MgCl_2$  at a flow rate of 0.75 ml/min. The molecular mass markers used were as follows: aldolase (158 kDa), bovine serum albumin (68 kDa), egg albumin (43 kDa), and trypsin inhibitor (23 kDa).

**CD Spectroscopy**—CD spectra were obtained with a Jasco J-600 automatic recording dichrograph at room temperature. A cell of 0.1 mm path length was used for the measurements in the far-UV region. CD data were expressed in terms of mean residue ellipticity,  $[\theta]$ , using the mean residue molecular mass of 114.6 calculated from the amino acid sequence (25).

#### RESULTS

**Effects of Replacements on the Enzyme Activity**—The  $k_{cat}$  values of the wild-type and mutant PPases at pH 7.8 are shown in Table I. The plasmid-encoded wild-type PPase showed slightly higher enzyme activity than the authentic



PPase from cells (26). The replacement of Pro-39 with Ala resulted in enhancement of the catalytic activity, and P69A showed almost the same activity as the wild-type PPase. The enzyme activities of P14A, P43A, and P116A were considerably reduced, and their  $K_m$  values were about twice that of the wild-type enzyme. P100A, P104A, and P146A almost completely lost their enzyme activities, and the P72A variant was completely inactive.

The enzyme activities of the wild-type and variant PPases were measured at various pHs, from 5.5 to 10.0, as shown in Fig. 2. With the exception of P39A, P59A, and P116A, the variants showed almost the same pH-activity profile as the wild-type PPase; the maximum activity was observed between pH 7.5 and 9.0, and the activity decreased rapidly outside this pH range. P39A and P116A exhibited wide optimum pH ranges, with almost full activity even at pH 10.0. On the contrary, P59A had a narrow optimum pH range with the maximum activity at pH 8.0.

**Effects of Replacements on the Thermostability**—To examine the effects of the replacements on the thermostability of PS-3 PPase, the wild-type and variant PPases were incubated at 70°C for various times at a protein concentration of 1 mg/ml in 20 mM Tris-HCl buffer, pH 7.8, contain-

ing 5 mM MgCl<sub>2</sub>, and the enzyme activity remaining was measured at 37°C. The results are shown in Fig. 3. The wild-type PPase was thermostable, no loss of activity being observed after incubation for 1 h at 70°C in the presence of 5 mM MgCl<sub>2</sub>. The replacement of individual prolines with alanines affected the thermostability to varying degrees. As a whole, the thermostabilities of the variant PPases were related to their enzyme activities; the higher their enzyme activity was, the more thermostable they were, except for P116A, which was as thermostable as the wild-type PPase in spite of its low activity. P100A, P104A, and P146A, which were trimers before and after heat treatment, were thermolabile. The thermostability of P72A could not be examined by measuring the remaining activity after heat treatment since it was completely inactive.

**Effects of Replacements on the Subunit Assembly**—We previously found, through a study on its sedimentation coefficient, that PS-3 PPase exists as a trimer in the absence of Mg<sup>2+</sup> and as a hexamer in its presence (26). Thus, the effects of replacement of the prolines with alanines on the subunit assembly before and after incubation at 70°C for 1 h at a protein concentration of 1 mg/ml in the presence of 5 mM MgCl<sub>2</sub> were examined by measuring the molecular mass by HPLC-gel chromatography. The results are shown in Fig. 4. The wild-type PPase in the presence of 5 mM MgCl<sub>2</sub> was a hexamer, as reported, and incubation at 70°C for 1 h did not affect its subunit assembly. P116A was also a hexamer both before and after heat treatment, notwithstanding its considerably reduced enzyme activity. P39A and P69A, whose enzyme activities were almost the same as that of the wild-type PPase, also existed as a hexamer in the native state, but a small amount of trimer was observed for both variants after heating. For P59A, a considerable amount of trimer was observed after heat treatment, although it comprised only a hexamer before heat treatment. On the contrary, a small amount of trimer was observed in addition to a hexamer for the native states of P14A and P43A, and trimers were dominant after heat treatment. P100A, P104A, and P146A, whose enzyme activities were extremely low, were trimers both before and

TABLE I. Rate constants for the wild-type and variant PPases.

Strain	$k_{cat}$ (s <sup>-1</sup> )	$K_m$ (mM)	$k_{cat}/K_m$ (s <sup>-1</sup> ·mM <sup>-1</sup> )	Degree of conservation <sup>a</sup>
Wild-type	817.0	0.47	1,738.6	—
P14A	74.3	0.82	90.6	30 (Pr, A)
P39A	1,098.0	0.60	1,830.0	7 (Pr)
P43A	288.7	1.0	288.7	28 (Pr, Pl)
P59A	413.3	0.96	430.5	34 (Pr, Pl, A)
P69A	744.3	0.47	1,583.6	21 (Pr, Pl)
P72A	0	—	—	23 (Pr, Pl)
P100A	2.8	0.88	3.2	17 (Pr)
P104A	1.3	1.0	1.3	26 (Pr, Pl, A)
P116A	236.7	0.64	369.8	20 (Pr, Pl)
P146A	19.0	0.55	34.5	3 (PS-3, <i>Bst</i> , <i>Stu</i> )

<sup>a</sup>The number of PPases having a proline residue at the corresponding position in 37 family I PPases. Pr, prokaryote; Pl, plant; A, animal/fungi; PS-3, Thermophilic Bacterium PS-3; *Bst*, *Bacillus stearotherophilus*; *Stu*, *S. tubersum* (potato).

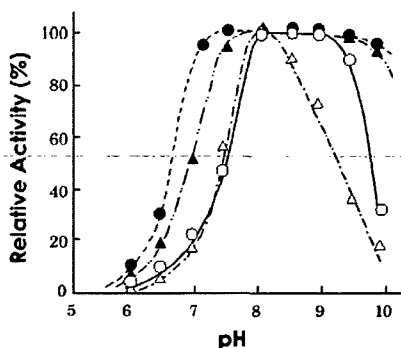


Fig. 2. Effect of pH on the catalytic activities of the wild-type and variant PPases from thermophilic bacterium PS-3. The activity of each enzyme at pH 7.8, at which all the PPases showed the maximum activity, was taken as 100%. The buffers used were 2-(*N*-morpholino)-ethane sulfonic acid (pH 5.5–7.0), Tris-HCl (pH 7.2–8.8), and glycine-NaOH (pH 9.0–10.5). ○, wild-type PPase; ●, P39A; △, P59A; ▲, P116A.

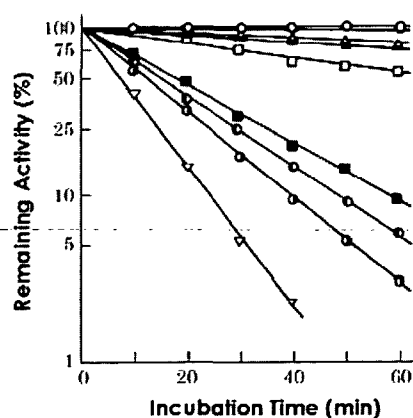


Fig. 3. Thermal inactivation of the wild-type and variant PPases from PS-3. The enzymes (1 mg/ml) in 20 mM Tris-HCl buffer, pH 7.8, containing 5 mM MgCl<sub>2</sub> were incubated at 70°C. Aliquots were withdrawn at the indicated times and assayed at 37°C. The enzyme activity without heating was taken as 100%. ○, wild-type PPase; ●, P116A; △, P69A; ▲, P39A; □, P59A; ■, P43A; ○, P14A; ○, P100A and P104A; ▽, P146A.

after heat treatment. Completely inactive P72A existed as a monomer before incubation at 70°C but was precipitated during heat treatment.

**CD Spectra**—In order to determine the effects of replacement of prolines with alanines on the protein conformation, CD spectra of the wild-type and variant PPases were measured at room temperature in the far-ultraviolet region

before and after incubation at 70°C for 1 h at the protein concentration of 1 mg/ml in the presence of 5 mM MgCl<sub>2</sub>. As shown in Fig. 5A, the CD bands of P72A and P146A before heat treatment were greatly reduced, indicating that the main-chain conformation of the wild-type PPase was partially disrupted by these replacements. The CD bands of P14A and P43A were also reduced slightly, and the remaining PPases exhibited almost the same CD spectra as the wild-type PPase.

Heat treatment did not affect the CD spectra of the wild-type, P39A, P69A, and P116A PPases; these three variant PPases exhibited almost identical spectra to that of the wild-type PPase before heat treatment. With the exception of P72A and P146A, the remaining variant PPases exhibited slightly reduced CD bands after heat treatment: the CD spectrum of P100A is shown in Fig. 5B as an example. P146A was profoundly influenced by heat treatment and its CD bands were further decreased (Fig. 5B). The CD spectrum of P72A could not be measured because of the precipitation during heat treatment.

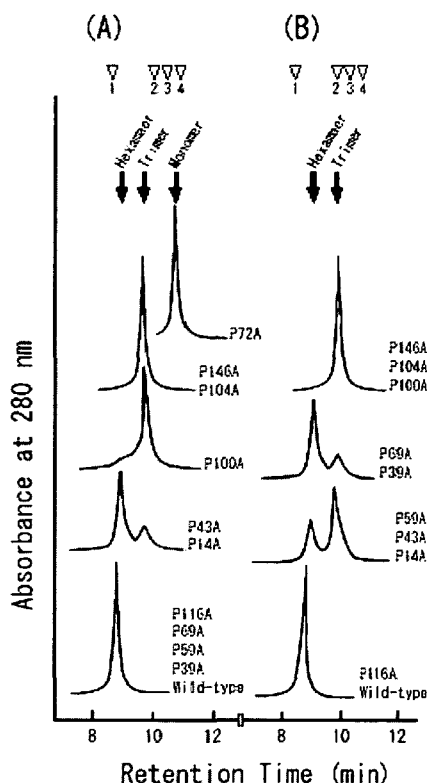


Fig. 4. HPLC-gel chromatography elution profiles of the PS-3 wild-type and variant PPases before (A) and after (B) incubation for 1 h at the protein concentration of 1 mg/ml at 70°C in the presence of 5 mM MgCl<sub>2</sub>. The buffer used was 20 mM Tris-HCl, pH 7.8, containing 5 mM MgCl<sub>2</sub>. The arrowheads (▽) indicate the elution positions of marker proteins: (1) aldolase (158 kDa), (2) bovine serum albumin (68 kDa), (3) egg albumin (43 kDa), and (4) trypsin inhibitor (23 kDa).

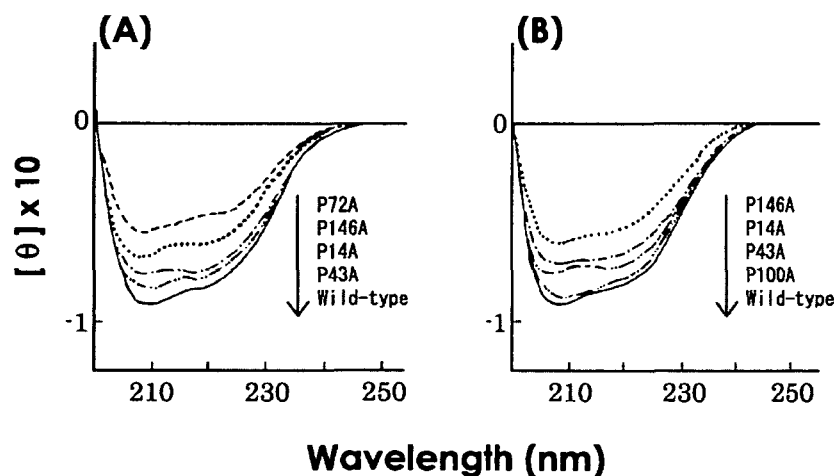


Fig. 5. CD spectra of the PS-3 wild-type and variant PPases before (A) and after (B) incubation for 1 h at 70°C at the protein concentration of 1 mg/ml in the presence of 5 mM MgCl<sub>2</sub>. The buffer used was 20 mM Tris-HCl, pH 7.8, and the measurements were carried out at room temperature.

## DISCUSSION

The variant most profoundly influenced by the replacement in the present study was P72A; it existed as a monomer even in the presence of Mg<sup>2+</sup> and completely lost its enzyme activity. Salminen *et al.* found, on analysis of the three-dimensional structures determined by X-ray crystallography, that residues Tyr-75 to Val-84 of *Eco* PPase are located at the protomer-protomer interface (34). Teplyakov *et al.* found that the interactions between subunits in the trimer of *Tth* PPase were very tight, which was due to four hydrogen bonds, including one between Pro-78 and Asn-28, together with the hydrophobic interactions of five residues in the region of Tyr-77 to Glu-86 and the parallel β bridge (30). Shinoda *et al.* deduced that the region Thr-66 to Asp-77 including Pro-72 in the *Bacillus stearothermophilus* (*Bst*) PPase was one of the protomer-protomer interfaces, by comparison of its primary structure with those of *Eco* and *Tth* PPases (35). They confirmed the importance of hydrophobic interaction(s) of Val-75 in this region for the trimer assembly through a study involving site-directed mutagenesis. The primary structure of PS-3 PPase is the same as that of *Bst* PPase except that the former has two

more amino acids at the C-terminus (25). Furthermore, Pro-72 and Asn-19 of PS-3 PPase correspond to Pro-78 and Asn-28 of *Tth* PPase, respectively, as judged from alignment of their primary structures; and the three-dimensional structure of PS-3 PPase, predicted by computer analysis of homology modeling, was very similar to those of both *Eco* and *Tth* PPases (Fig. 1).

Taking all these findings into account, the present findings strongly indicate that Pro-72 participates directly in the interaction between subunits in the trimer. Moreover, Pro-72 might play an important role in the conformational integrity of PS-3 PPase, because its replacement also resulted in remarkable reduction of the CD bands in the far-ultraviolet region, and precipitation at high temperature. Most of the prokaryotic and plant PPases whose primary structures have been determined (23 out of 28 PPases) have a proline residue at the position corresponding to Pro-72 of PS-3 PPase. Thus, a proline residue at this position might also play an important role in these PPases.

Shinoda *et al.* pointed out that Pro-100 and Pro-104, which are specific for prokaryotic PPases, could also be located at another protomer-protomer interface in *Bst* PPase (35). For P100A and P104A, however, only a trimer, not a monomer, was observed accompanying the considerably reduced enzyme activity, indicating that the region containing Pro-100 and Pro-104 might not directly contribute to the protomer-protomer association, but it might be structurally important for the trimer-trimer association due to Mg<sup>2+</sup>.

Another variant profoundly influenced by the replacement was P146A. Pro-146 is only found in the PS-3, *Bst* and *S. tuberosum* PPase among 37 Family I PPases (7) and is deduced to be located at the beginning of Helix B from Fig. 1. Its replacement with Ala resulted in almost complete disappearance of the enzyme activity, and remarkable reductions of the CD bands in the far-ultraviolet region were also observed, indicating that the backbone structure was considerably destroyed. P146A was a trimer before and after heat treatment even in the presence of Mg<sup>2+</sup>. The breakdown of backbone structure, probably Helix B, by replacement of Pro-146 with Ala might influence the overall structure, which would lead to the inability of trimers to associate into hexamers. Thus, Pro-146, a residue characteristic of PS-3 PPase, seems to be important for the overall integrity of the protein molecule.

The replacement of Pro-116, which is located just before Helix A, gave a contradictory result. Most of the prokaryotic and plant PPases have a proline at the corresponding position of P-116 of PS-3 PPase. Although the enzyme activity of P116A was about half that of the wild-type PPase, it was a hexamer before and after heat treatment in the presence of Mg<sup>2+</sup> and showed an almost identical CD spectrum in the far-ultraviolet region to that of the wild-type PPase, which did not change on heat treatment.

Pro-14, Pro-43, and Pro-59, the positions corresponding to which in most soluble PPases are also occupied by prolines, are located very near to or in the cluster of putative active-site residues (Glu-12, Tyr-42, Asp-56, Asp-58, and Asp-61). Therefore, the replacement of these proline residues might influence the three-dimensional arrangement of the active-site residues, which would result in a reduction of the enzyme activity. The replacement of Pro-39 and Pro-69 did not influence the subunit assembly in the presence

of Mg<sup>2+</sup>, and the enzyme activities of both variants were almost the same as that of the wild-type PPase. Only 7 prokaryotic PPases out of 37 soluble PPases have a proline at the position corresponding to Pro-39 of PS-3 PPase, whereas 21 prokaryotic and plant PPases have a proline at the position corresponding to Pro-69. However, both Pro-39 and Pro-69 are located relatively far from the active-site pocket and on the surface of the protein molecule. Therefore, these two proline residues might not play important roles in the integrity of protein molecule.

The results of the present study indicate that, with some exceptions, most of the proline residues in PS-3 PPase play very important roles, and some of them are critical for the integrity of the protein molecule. The present results also indicate that the thermostability of PS-3 PPase is profoundly related with its subunit structure. The catalytic activity after heat treatment seemed to be proportional to the amount of hexamer remaining, although CD spectra indicated that the backbone structure was not affected by heat treatment, even for the trimer. On the contrary, the monomer was less stable and precipitated on heat treatment. Thus, protomer-protomer interactions as well as trimer-trimer ones seem to be important for maintenance of the correct structure, which is necessary for the catalytic activity and thermostability. Leppanen *et al.* (29) and Teplyakov *et al.* (30) also reported that the tightly packed hexameric structure that increases the surface area of the trimer-trimer interface, which is characteristic of *Tth* and *Sac* PPases, is important for the thermostability of these two highly thermostable PPases.

## REFERENCES

1. Kornberg, A. (1962) On the metabolic significance of phospholytic and pyrophospholytic reactions in *Horizons in Biochemistry* (Kasha, H. and Pullman, P., eds.) pp. 251–264, Academic Press, New York
2. Lahti, R. (1983) Microbial inorganic pyrophosphatase. *Microbiol. Rev.* **47**, 169–179
3. Baykov, A.A., Cooperman, B.S., Goldman, A., and Lahti, R. (1999) Cytoplasmic inorganic pyrophosphatase. *Prog. Mol. Subcell. Biol.* **23**, 127–150
4. Chen, J., Brevet, A., Fromant, M., Leveque, F., Schmitter, J.-M., Blanquet, S., and Plateau, P. (1990) Pyrophosphatase is essential for growth of *Escherichia coli*. *J. Bacteriol.* **172**, 5686–5689
5. Lundin, M., Baltscheffsky, H., and Ronne, H. (1991) Yeast *PPA2* gene encodes a mitochondrial inorganic pyrophosphatase that is essential for mitochondrial function. *J. Biol. Chem.* **266**, 12168–12172
6. Sonnewald, U. (1992) Expression of *E. coli* inorganic pyrophosphatase in transgenic plants alters photo-assimilate partitioning. *Plant J.* **2**, 571–581
7. Sivula, T., Salminen, A., Parfenyev, A.N., Pohjanjoki, P., Goldman, A., Cooperman, B.S., Baykov, A.A., and Lahti, R. (1999) Evolutionary aspect of inorganic pyrophosphatase. *FEBS Lett.* **454**, 75–80
8. Shintani, T., Uchiumi, T., Yonezawa, T., Salminen, A., Baykov, A.A., Lahti, R., and Hachimori, A. (1998) Cloning and expression of a unique inorganic pyrophosphatase from *Bacillus subtilis*: evidence for a new family of enzymes. *FEBS Lett.* **439**, 263–266
9. Young, T.W., Kuhn, N.J., Wadson, A., Ward, S., Burges, D., and Cooke, G.D. (1998) *Bacillus subtilis* ORF yybQ encodes a manganese-dependent inorganic pyrophosphatase with distinctive properties: the first of a new class of soluble pyrophosphatase? *Microbiology* **144**, 2563–2571
10. Kuhn, N.J., Wadson, A., Ward, S., and Young, T.W. (2000)

- Methanococcus jannaschii* ORF mj0608 codes for a class C inorganic pyrophosphatase protected by  $\text{Co}^{2+}$  or  $\text{Mn}^{2+}$  ions against fluoride inhibition. *Arch. Biochem. Biophys.* **379**, 292–298
11. Parfenyev, A.N., Salminen, A., Halonen, P., Hachimori, A., Baykov, A.A., and Lahti, R. (2001) Quaternary structure and metal ion requirement of Family II pyrophosphatase from *Bacillus subtilis*, *Streptococcus gordonii* and *Streptococcus mutans*. *J. Biol. Chem.* **276**, 24511–24518
  12. Kankare, J., Neal, G.S., Salminen, T., Glumoff, T., Cooperman, B.S., Lahti, R., and Goldman, A. (1994) The structure of *E. coli* soluble inorganic pyrophosphatase at 2.7 Å resolution. *Protein Eng.* **7**, 823–830
  13. Kankare, J., Salminen, T., Lahti, R., Cooperman, B.S., Baykov, A.A., and Goldman, A. (1996) Crystallographic identification of metalbinding sites in *Escherichia coli* inorganic pyrophosphatase. *Biochemistry* **35**, 4670–4677
  14. Heikinheimo, P., Lehtonen, J., Baykov, A.A., Lahti, R., Cooperman, B.S., and Goldman, A. (1996) The structural basis for pyrophosphatase catalysis. *Structure* **4**, 1491–1508
  15. Harutyunyan, E.H., Kuranova, I.P., Vainshtein, B.K., Höhne, W.E., Lamzin, V.S., Dauter, Z., Teplyakov, A.V., and Wilson, K.S. (1996) X-ray structure of yeast inorganic pyrophosphatase complexed with manganese and phosphate. *Eur. J. Biochem.* **239**, 220–228
  16. Harutyunyan, E.H., Oganessyan, V.Yu., Oganessyan, N.N., Avaeva, S.M., Nazarova, T.I., Vorobyeva, N.N., Kurilova, S.A., Huber, R., and Mather, T. (1997) Crystal structure of holo inorganic pyrophosphatase from *Escherichia coli* at 1.9 Å resolution. Mechanism of hydrolysis. *Biochemistry* **36**, 7754–7760
  17. Salminen, T., Käpylä, J., Heikinheimo, P., Kankare, J., Goldman, A., Heinonen, J., Baykov, A.A., Cooperman, B.S., and Lahti, R. (1995) Structure and function analysis of *Escherichia coli* inorganic pyrophosphatase: is a hydroxide ion the key to catalysis? *Biochemistry* **34**, 782–791
  18. Pohjanjoki, P., Lahti, R., Goldman, A., and Cooperman, B.S. (1998) Evolutionary conservation of enzymatic catalysis: quantitative comparison of the effects of mutation of aligned residues in *Saccharomyces cerevisiae* and *Escherichia coli* inorganic pyrophosphatases on enzymatic activity. *Biochemistry* **37**, 1754–1761
  19. Käpylä, J., Hyytiä, T., Lahti, R., Goldman, A., Baykov, A.A., and Cooperman, B.S. (1995) Effect of D97E substitution on the kinetic and thermodynamic properties of *Escherichia coli* inorganic pyrophosphatase. *Biochemistry* **34**, 792–800
  20. Volk, S.E., Dudarenkov, V.Y., Käpylä, J., Kasho, V.N., Voloshina, O.A., Salminen, T., Goldman, A., Lahti, R., Baykov, A.A., and Cooperman, B.S. (1996) Effect of E20D substitution in the active site of *Escherichia coli* inorganic pyrophosphatase on its quaternary structure and catalytic properties. *Biochemistry* **35**, 4662–4669
  21. Avaeva, S., Rodina, E., Kurilova, S.A., Nazarova, T.I., and Vorobyeva, N.N. (1996) Effect of D42N substitution in *Escherichia coli* inorganic pyrophosphatase on catalytic activity and  $\text{Mg}^{2+}$  binding. *FEBS Lett.* **392**, 91–94
  22. Avaeva, S., Ignatov, P., Kurilova, S.A., Nazarova, T.I., Rodina, E., Vorobyeva, N., Oganessyan, V., and Harutyunyan, E. (1996) *Escherichia coli* inorganic pyrophosphatase: site-directed mutagenesis of the metal binding sites. *FEBS Lett.* **399**, 99–102
  23. Fabrichniy, L., Kasho, V., Hyytiä, T., Salminen, T., Halonen, P., Dudarenkov, V., Heikinheimo, P., Chernyak, V., Goldman, A., Lahti, R., Cooperman, B.S., and Baykov, A.A. (1997) Structural and functional consequences of substitutions at the tyrosine 55-lysine 104 hydrogen bond in *Escherichia coli* inorganic pyrophosphatase. *Biochemistry* **36**, 7746–7753
  24. Ichiba, T., Takenaka, O., Samejima, T., and Hachimori, A. (1990) Primary structure of the inorganic pyrophosphatase from thermophilic bacterium PS-3. *J. Biochem.* **108**, 572–578
  25. Maruyama, S., Maeshima, M., Nishimura, M., Aoki, M., Ichiba, T., Sekiguchi, J., and Hachimori, A. (1996) Cloning and expression of the inorganic pyrophosphatase gene from thermophilic bacterium PS-3. *Biochem. Mol. Biol. Int.* **406**, 79–88
  26. Hachimori, A., Shiroya, Y., Hirato, A., Miyahara, T., and Samejima, T. (1979) Effects of divalent cations on thermophilic inorganic pyrophosphatase. *J. Biochem.* **86**, 121–130
  27. Aoki, M., Uchiumi, T., Tsuji, E., and Hachimori, A. (1998) Effects of replacement of His-118, His-125 and Trp-143 by alanine on the catalytic activity and subunit assembly of inorganic pyrophosphatase from thermophilic bacterium PS-3. *Biochem. J.* **331**, 143–148
  28. Matthews, B.W., Nicholson, H., and Becktel, W.J. (1987) Enhanced protein thermostability from site-directed mutations that decrease the entropy of unfolding. *Proc. Natl. Acad. Sci. USA* **84**, 6663–6667
  29. Leppanen, V. M., Nummelin, H., Hansen, T., Lahti, R., Schäfer, G., and Goldman, A. (1999) *Sulfolobus acidocaldarius* inorganic pyrophosphatase: structure, thermostability, and effect of metal ion in an archaeal pyrophosphatase. *Protein Sci.* **8**, 1218–1231
  30. Teplyakov, A., Obmolova, G., Wilson, K.S., Ishii, K., Kaji, H., Samejima, T., and Kuranova, I. (1994) Crystal structure of inorganic pyrophosphatase from *Thermus thermophilus*. *Protein Sci.* **3**, 1098–1107
  31. Sanger, F., Nicklen, S., and Coulson, A.R. (1981) DNA sequencing with chain-terminating inhibitors. *Proc. Natl. Acad. Sci. USA* **74**, 5463–5467
  32. Hachimori, A., Takeda, A., Kaibuchi, M., Ohkawara, N., and Samejima, T. (1975) Purification and characterization of inorganic pyrophosphatase from *Bacillus stearothermophilus*. *J. Biochem.* **77**, 1177–1183
  33. Peel, J.L. and Loughman, B.C. (1957) Some observations on the role of copper ions in the reduction of phosphomolybdate by ascorbic acid and their application in the determination of inorganic phosphate. *Biochem. J.* **65**, 709–716
  34. Salminen, T., Teplyakov, A., Kankare, J., Cooperman, B.S., Lahti, R., and Goldman, A. (1996) An unusual route to thermostability disclosed by the comparison of *Thermus thermophilus* and *Escherichia coli* inorganic pyrophosphatases. *Protein Sci.* **5**, 1014–1025
  35. Shinoda, H., Hattori, M., Shimizu, A., Samejima, T., and Satoh, T. (1999) Hydrophobic interactions of Val-75 are critical for oligomeric thermostability of inorganic pyrophosphatase from *Bacillus stearothermophilus*. *J. Biochem.* **125**, 58–63